

JLab: Probing Hadronic Physics with Electrons and Photons

Elton S. Smith

Thomas Jefferson National Accelerator Facility, Newport News, Virginia 23606, USA

Received on 11 September, 2003

Precision measurements of the structure of nucleons and nuclei in the regime of strong interaction QCD are now possible with the availability of high current polarized electron beams, polarized targets, and recoil polarimeters, in conjunction with modern spectrometers and detector instrumentation. The physics at JLab will be highlighted using two recent measurements of general interest. The ratio of the proton electric to magnetic form factors indicates the importance of the role of angular momentum in the structure of the nucleon. The existence of 5-quark configurations in the ground state wavefunctions of hadrons is confirmed by a narrow peak attributed to an exotic baryon with strangeness $S=+1$. These and other examples will be used to illustrate the capabilities and focus of the experimental program at JLab.

1 Introduction to JLab

The Continuous Electron Beam Accelerator Facility (CEBAF) at the Thomas Jefferson National Accelerator Facility (Jefferson Lab) is devoted to the investigation of the electromagnetic structure of mesons, nucleons, and nuclei using high energy and high duty-cycle electron and photon beams.

CEBAF is a superconducting electron accelerator with an initial maximum energy of 4 GeV and 100 % duty-cycle. Three electron beams with a maximum total current of 200 μA can be used simultaneously for electron scattering experiments in the experimental areas, Halls A, B, and C. The accelerator design concept is based on two parallel superconducting continuous-wave linear accelerators joined by magnetic recirculation arcs. The accelerating structures are five-cell superconducting niobium cavities with a nominal average energy gain of 5 MeV/m. The accelerator performance has met all design goals, achieving 5.7 GeV for physics running, and delivering high quality beams with intensity ratios exceeding $10^6:1$. The electron beam is produced using a strained GaAs photocathode delivering polarized electrons ($P_e \geq 75\%$) simultaneously to all three halls.

Three experimental areas are available for simultaneous experiments, the only restriction being that the beam energies have to be multiples of the single pass energy. The halls contain complementary equipment which cover a wide range of physics topics: Hall A has two high resolution magnetic spectrometers with 10^{-4} momentum resolution in a 10% momentum bite, and a solid angle of 8 msr. Hall B houses the large acceptance spectrometer, CLAS [1]. Hall C uses a combination of a high momentum spectrometer (10^{-3} momentum resolution, 7 msr solid angle and maximum momentum of 7 GeV/c) and a short orbit spectrometer.

To illustrate the physics which is being addressed at Jefferson Lab, we have chosen two topics of current interest: measurements of the electric form factor of the proton in Hall A, and the observation of an exotic $S=+1$ baryon with the CLAS.

2 The shape of the proton at high Q^2

Electron scattering is the tool of choice for the precise investigation of the spatial structure of nucleons and nuclei. The precision arises from the well-known characteristics of the electromagnetic interaction. By varying the momentum transferred from the electron to the target for fixed excitation energy, we can directly map out the charge and current densities, and the transition densities associated with its excitation [2]. In the non-relativistic limit and for small four-momentum transfer squared, Q^2 , the electric (G_{Ep}) and magnetic (G_{Mp}) form factors are given by the Fourier transforms of the charge and current distributions in the nucleon. As Q^2 increases, the proton exhibits its internal structure as a multi-body relativistic system of quarks and gluons.

The unpolarized elastic ep cross section is given by:

$$\frac{d\sigma}{d\Omega} = \frac{\alpha^2 \cos^2 \frac{\theta_e}{2}}{4E_e^2 \sin^4 \frac{\theta_e}{2}} \frac{E_{e'}}{E_e} \left(\frac{1}{1+\tau} \right) \left[G_{Ep}^2 + \frac{\tau}{\epsilon} G_{Mp}^2 \right] \quad (1)$$

where E_e is the beam energy, $E_{e'}$ and θ_e are the energy and angle of the scattered electron, the polarization of the virtual photon is $\epsilon = [1 + 2(1+\tau) \tan^2 \frac{\theta_e}{2}]^{-1}$, and $\tau = Q^2/4M_p^2$ is the four momentum scaled to the proton mass. The Rosenbluth method uses Eq. (1) to determine the individual contributions from G_{Ep} and G_{Mp} by using their kinematic dependence on ϵ at fixed Q^2 . The world data for the electric and magnetic form factors prior to 1998 is shown in Fig. 1. The form factors are found empirically to approximately follow the dipole form G_D which is used as a reference:

$$G_{Ep} \sim \frac{G_{Mp}}{\mu_p} \sim G_D = \frac{1}{\left(1 + \frac{Q^2}{0.71}\right)} \quad (2)$$

In the non-relativistic limit, the dipole shape corresponds to an exponential charge distribution.

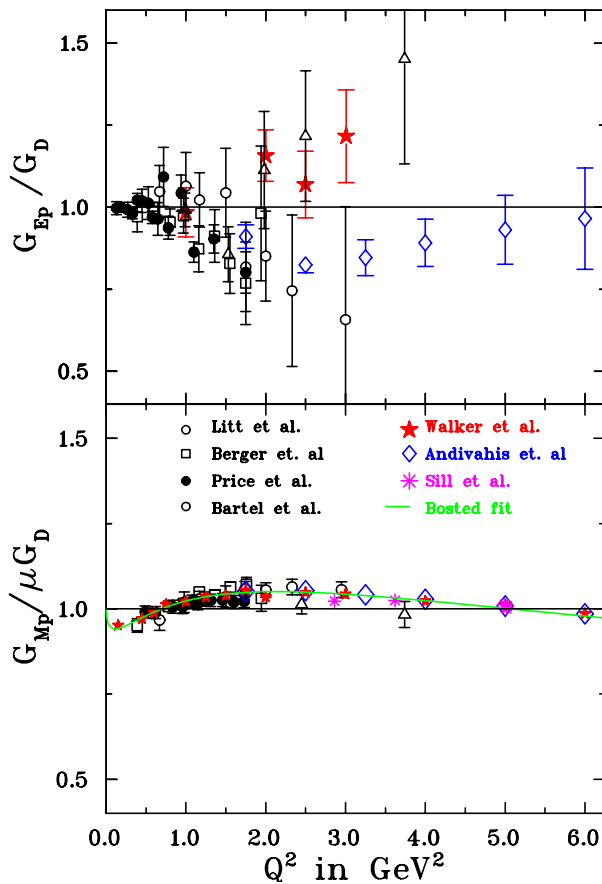


Figure 1. World data prior to 1998 for G_{Ep}/G_D (top) and $G_{Mp}/\mu_p G_D$ (bottom).

At high Q^2 the cross section is dominated by the magnetic term G_{Mp} , which makes the determination of the electric form factor G_{Ep} by the Rosenbluth method increasingly difficult.

Measurements of the ratio of G_{Ep}/G_{Mp} have been completed at Jefferson Lab for Q^2 between 0.5 and 5.6 GeV^2 by measuring the polarization of the recoil proton in $\bar{e}p \rightarrow e\bar{p}$ scattering [3, 4]. The scattering of longitudinally polarized electrons on unpolarized protons results in a transfer of polarization to the recoil proton with two components in the scattering plane: P_t is perpendicular and P_l is the parallel to the proton momentum. The polarization of the proton is determined using a polarimeter with a graphite or CH_2 analyzer located at the focal plane of the proton spectrometer. The ratio of electric to magnetic form factors is directly proportional to the ratio of polarizations:

$$\frac{G_E^p}{G_M^p} = -\frac{P_t}{P_l} \frac{E_e + E_{e'}}{2M_p} \tan\left(\frac{\theta_e}{2}\right) \quad (3)$$

In first order the polarization normal to the scattering plane is zero and can serve as a systematic check.

Since the ratio G_E^p/G_M^p is accessed directly, these experiments are able to carefully control their systematic uncertainties. For example, the ratio is independent of the electron beam polarization and the analyzing power of the polarimeter. Also, detailed knowledge of the spectrometer acceptances are not needed; the dominant systematic error

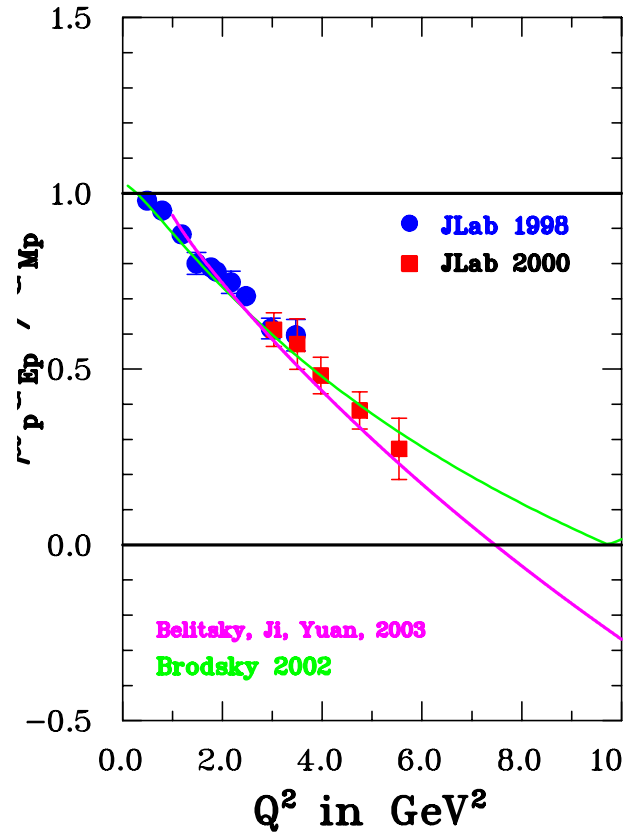


Figure 2. JLab measurements for the ratio $\mu_p G_{Ep}/G_{Mp}$ as a function of Q^2 , determined by measuring the recoil proton polarization. The curves are described in the text.

comes from uncertainties in calculating the transport of the spin through the magnet.

The results of these measurements are shown in Fig. 2 as the ratio $\mu_p G_{Ep}/G_{Mp}$. The plot demonstrates the somewhat surprising result that the form factor ratio decreases linearly with increasing Q^2 , and will cross zero at $Q^2 \approx 7.5 \text{ GeV}^2$ if the trend continues. The data have motivated a flurry of theoretical activity. The leading-order pQCD predicts that the ratio of Pauli to Dirac form factors should scale as $F_2/F_1 \sim 1/Q^2$. If logarithmic corrections are included to the leading-order prediction, the ratio behaves more like $F_2/F_1 \sim 1/Q$ [5, 6] and the calculations reproduce the data by adjusting appropriate parameters as shown in Fig. 2. The behavior of the data requires that the quarks inside the proton carry orbital angular momentum [7, 8].

These new data on G_{Ep} have motivated discussions regarding their physical interpretation in terms of the shape of the proton [9, 10, 11]. The calculations have been used to produce images of the proton by selecting specific configurations of the quark momenta and spins. When viewed through these “color” filters to select specific quark configurations, the shape of the proton becomes non-spherical. We await new data to probe deeper into the structure of the proton. The experiment is approved to extend measurements up to a momentum transfer of 9 GeV/c^2 [12].

3 Pentaquarks

The question of which color singlet configurations exist in nature lies at the heart of strong interaction QCD. Until recently all experimental evidence indicated that mesons were ($q\bar{q}$) bound states and the valence structure of baryons was (qqq). In the baryon sector, it is natural to ask whether a 5-quark configurations exists where the \bar{q} has a different flavor than (and hence cannot annihilate with) the other four quarks. A baryon with the exotic strangeness quantum number $S = +1$ is a natural candidate for a pentaquark state, because such a state has a minimal 5-quark ($qqqq\bar{q}$) configuration. Such states are not forbidden [13, 14], and definite evidence of pentaquark states would be an important addition to our understanding of QCD.

Pentaquark states have been studied both theoretically and experimentally for many years [15]. Most recently, symmetries within the chiral soliton model were used by Diakonov, Petrov and Polyakov [16] to predict an anti-decuplet of 5-quark resonances with spin and parity $J^\pi = \frac{1}{2}^+$. The lowest mass member, now called the Θ^+ , is an isosinglet with valence quark configuration $uudd\bar{s}$ giving strangeness $S = +1$ with a predicted mass of approximately 1.53 GeV/c² and a width of ~ 0.015 GeV/c². These definite predictions have prompted experimental searches to focus attention in this mass region.

This paper describes the evidence for a narrow $S = +1$ baryon observed in the reaction $\gamma d \rightarrow K^+K^-p(n)$ using the CLAS detector in Hall B [17]. However, several other experiments have reported evidence for a state at the same mass. The first observation of an $S = +1$ baryon was reported by the LEPS collaboration at the SPring-8 facility in Japan at a mass of 1.54 GeV/c², decaying to nK^+ with a FWHM less than 0.025 GeV/c² [18]. Confirming evidence has also come from the DIANA collaboration at ITEP [19] in the K^0p mass spectrum, the SAPHIR collaboration in photoproduction on a proton [20], and most recently a peak in the pK_s^0 system was reported in neutrino and antineutrino interactions on nuclei [21].

The CLAS data was taken with a photon beam which was produced by 2.474 and 3.115 GeV electrons incident on a bremsstrahlung radiator of thickness 10^{-4} radiation lengths, giving a tagged photon flux of approximately 4×10^6 γ 's per second. The photons were incident on a 10-cm long liquid-deuterium target. The event trigger required a single charged track in CLAS in coincidence with a hit in the tagging spectrometer. The momentum of charged particles were reconstructed using magnetic analysis and their mass determined using time-of-flight techniques. The analysis selected events with a detected proton, K^+ and K^- in the final state, all of which originated from the same beam bucket. The detection of all three charged particles allows complete determination of the reaction and therefore Fermi motion in the target plays no role in the analysis. The missing mass (MM) of the selected events is plotted in Fig. 3, which shows clear peak at the the neutron mass. A fit to the distribution (solid line) yields a mass resolution of $\sigma = 0.009$ GeV/c². Events within $\pm 3\sigma$ of the neutron peak were kept for further analysis. The background in this region is about

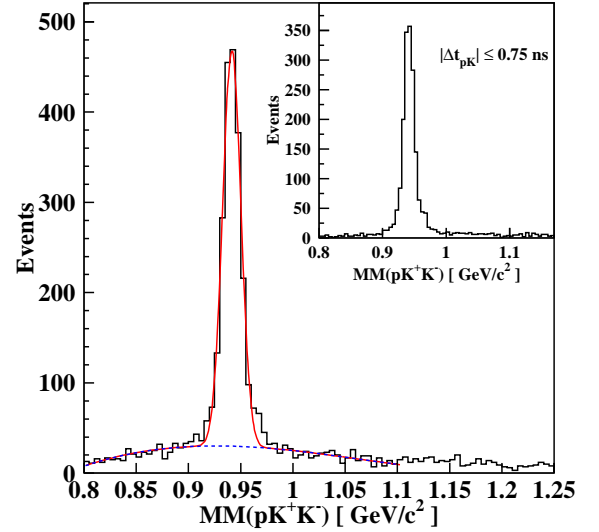


Figure 3. Missing mass spectrum for the $\gamma d \rightarrow pK^+K^-X$ reaction, after timing cuts to identify the charged particles and the coincident photon, which shows a peak at the neutron mass. There is a small, broad background from misidentified particles and other sources. The inset shows the neutron peak with a tighter requirement on the timing between the proton and kaons.

15% of the total, mostly from pions that are misidentified as kaons. A cleaner spectrum can be obtained by applying tighter timing cuts (as shown in the inset), but at the expense of reducing the signal.

Several additional cuts were made to optimize the selection of the final sample. First we required that the reconstructed neutron momentum be greater than 0.08 GeV/c². This selection enhances the number interactions where the neutron participates to produce a Θ^+ , and is not a spectator. There are several known resonances which result in the same final state and we explicitly removed the two strongest, the ϕ meson at 1.02 GeV/c² and the $\Lambda(1520)$. A final cut removed events with K^+ whose momenta exceeds 1.0 GeV/c, which are associated with invariant masses of the nK^+ system above ~ 1.7 GeV/c².

The final nK^+ invariant mass spectrum, $M(nK^+)$, is shown in Fig. 4. The spectrum of events removed by the $\Lambda(1520)$ cut is also shown in Fig. 4 by the dashed-dotted histogram, and does not appear to be associated with the peak at 1.54 GeV/c². The number of events in the peak was estimated using several assumptions for the shape of the background. The solid line fit in the figure uses an empirical Gaussian plus constant term for the background (dashed line). This fit determines 43 counts in the peak at a mass of 1.542 ± 0.005 GeV/c² with a width (FWHM) of 0.021 GeV/c². The dotted line shows a background shape based on a linear combination of 4-body phase space and 3-body phase space of the pK^+K^- final state (K^+K^- in s-wave). The phase space distributions were generated using a GEANT-based Monte Carlo followed by the same reconstruction package as the real data.

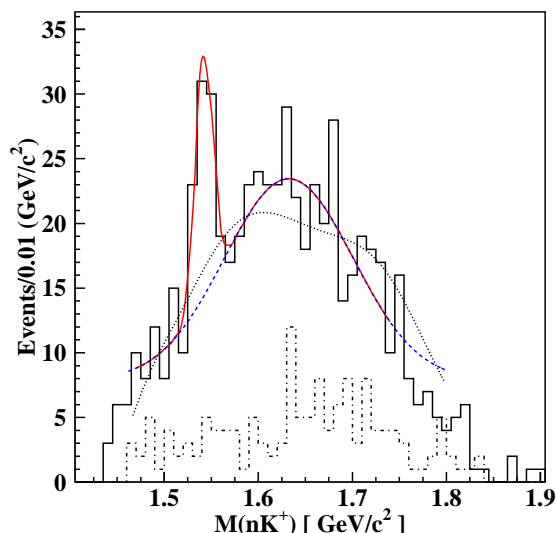


Figure 4. Invariant mass of the nK^+ system, which has strangeness $S = +1$, showing a sharp peak at the mass of $1.542 \text{ GeV}/c^2$. The dashed-dotted histogram shows the spectrum of events associated with $\Lambda(1520)$ production. See text for explanation of the background shapes.

To determine the sensitivity of our experiment, which depends on the actual shape of the background, ten combinations of cut placements and fitting functions were tried. The estimated statistical significance in those ten cases ranges from 4.6σ to 5.8σ , which we use to derive the conservative estimate for the statistical significance of our result of $5.2 \pm 0.6 \sigma$.

In summary, evidence is mounting for the existence of a baryon with a minimum content of 5-quarks. However, the properties of this $S = +1$ state, such as spin, isospin and parity, still need to be determined before it can be conclusively identified with the Θ^+ predicted in Ref. [16]. In addition to this baryon, we expect a whole families of pentaquarks which promise to rewrite our understanding of baryon spectroscopy. The implications of this discovery are being evaluated continuously in the literature [22] and we can only expect more surprises in the near future.

Acknowledgments

I would like to thank R.V. Ribas, and all organizers of the conference, for their gracious hospitality. I would also like to thank C.F. Perdrisat, V. Punjabi and E. Brash for their assistance in preparation of the material on the proton electric form factor, and to S. Stepanyan for help in the preparation of materials on the pentaquark. The Southeastern Universities Research Association (SURA) operates the Thomas

Jefferson National Accelerator Facility for the U.S. Department of Energy under contract DE-AC05-84ER40150.

References

- [1] B.A. Mecking *et al.*, Nucl. Instr. Meth. A **503**, 513 (2003).
- [2] E.J. Brash, "Nucleon Electromagnetic Form Factors," p. 256 Baryons 2002, Jefferson Lab, March 3-8, 2002.
- [3] M.K. Jones *et al.*, Phys. Rev. Lett. **84**, 1398 (2000).
- [4] O. Gayou *et al.*, Phys. Rev. Lett. **88**, 092301 (2002).
- [5] S.J. Brodsky, "Perspectives on Exclusive Processes in QCD," Workshop on Exclusive Processes at High Momentum Transfer, Jefferson Lab, May 15-18, 2002 hep-ph/0208158.
- [6] A.V. Belitsky, X. Ji and F. Yuan, Phys. Rev. Lett. **91**, 092003 (2003) hep-ph/0212351.
- [7] P. Jain and J.P. Ralston, hep-ph/0306194 (2003).
- [8] G.A. Miller and M.R. Frank, Phys. Rev. C **65**, 065205 (2002).
- [9] G.A. Miller, "The Shape of the Proton," nucl-th/0304076 v2 (2003).
- [10] A.V. Belitsky, X. Ji and F. Yuan, "Quark Imaging in the Proton Via Quantum Phase-Space Distributions," hep-ph/0307383 (2003).
- [11] X. Ji, Phys. Rev. Lett. **91**, 062001-1 (2003).
- [12] For a recent review of these measurements, see V. Punjabi and C.F. Perdrisat, nucl-ex/0307001 (2003), and references therein.
- [13] D. Strottman, Phys. Rev. D **20**, 748 (1979).
- [14] H.J. Lipkin, Nucl. Phys. A **625**, 207 (1997).
- [15] Particle Data Group, Phys. Lett. B **170**, 289 (1986).
- [16] D. Diakonov, V. Petrov, and M. Polyakov, Z. Phys. A **359**, 305 (1997).
- [17] S. Stepanyan (The CLAS Collaboration), arXiv:hep-ex/0307018
- [18] T. Nakano (The LEPS Collaboration) *et al.*, Phys. Rev. Lett. **91**, 012002 (2003) [arXiv:hep-ex/0301020]
- [19] V.V. Barmin *et al.* (The DIANA Collaboration), Phys. At. Nucl., **66**, 1715 (2003) [arXiv:hep-ex/0304040]
- [20] J. Barth *et al.* (The SAPHIR Collaboration), arXiv:hep-ex/0307083
- [21] A.E. Asratyan *et al.*, submitted to Yad. Fiz., arXiv:hep-ex/0309042.
- [22] For a review of the phenomenology and models, see B. Jennings and K. Maltman, hep-ph/0308286